Electronic Supplementary Information (ESI) for:

Nanotransfer printing of plasmonic nano-pleat arrays with ultra-reduced nanocavity width using perfluoropolyether molds

Chia-Ching Liang,[a] *Wen-Huei Chang,*[b] *and Chun-Hung Lin*[*a,c,d]

[a] Department of Photonics, National Cheng Kung University, Tainan 701, Taiwan.
[b] Department of Applied Chemistry, National Pingtung University, Pingtung 900, Taiwan.
[c] Center for Micro/Nano Science and Technology, National Cheng Kung University, Tainan 701, Taiwan.
[d] Advanced Optoelectronic Technology Center, National Cheng Kung University, Tainan 701, Taiwan
[*] E-mail address: chlin@mail.ncku.edu.tw

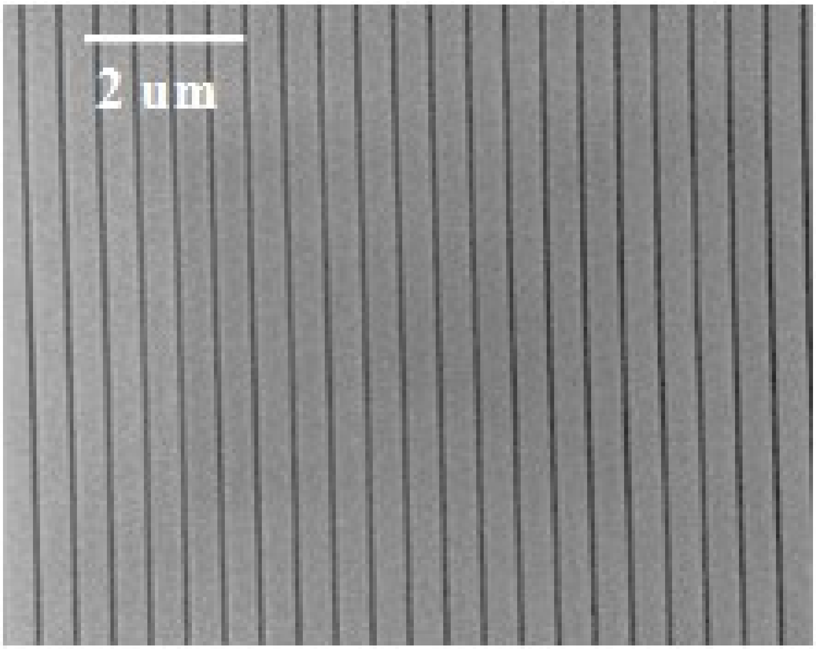

Fig. S1 SEM image of a gold nano-pleat array transferred from a re-used PFPE mold.

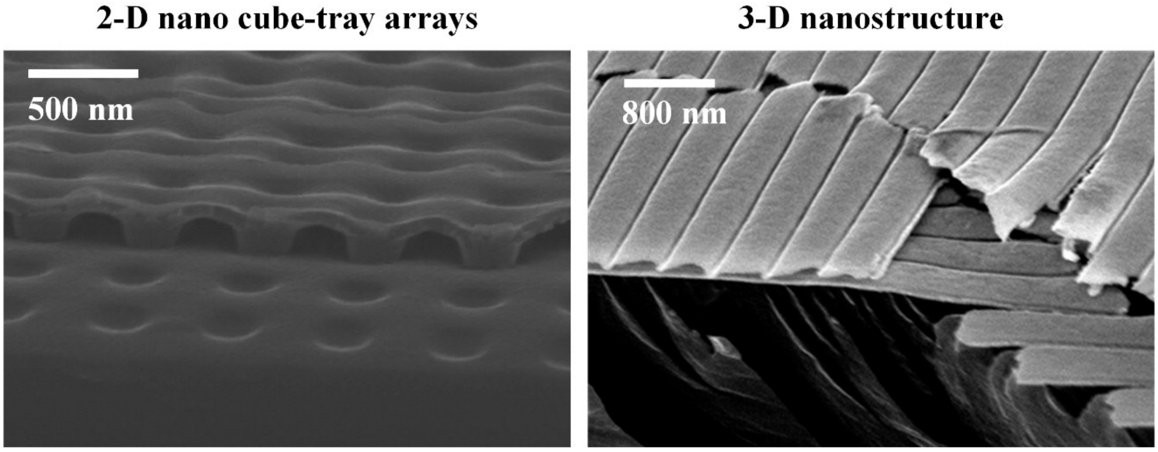

(a) (b)

Fig. S2 SEM images of (a) a 2D nano cube-tray array and (b) a multilayer 3D nanostructure.

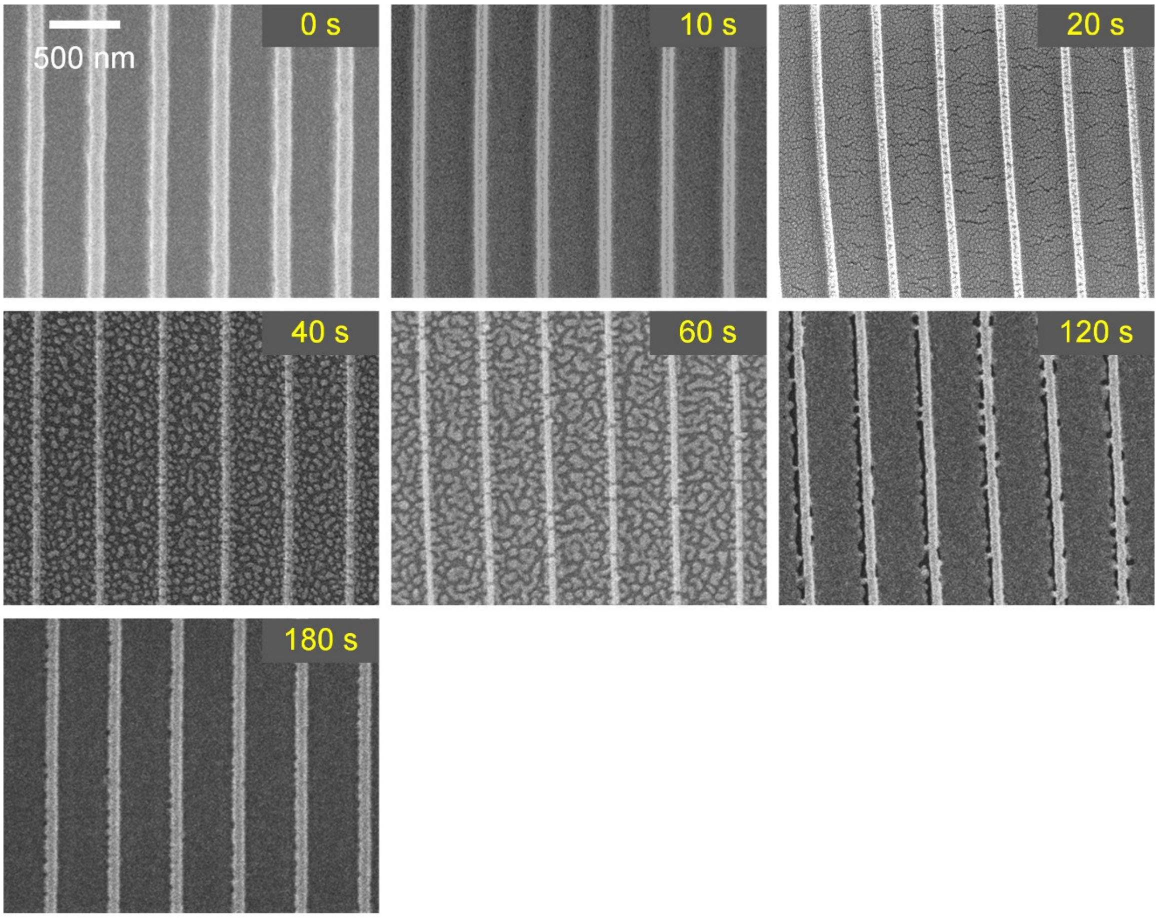

Fig. S3 Top-view SEM images of the deposited gold on PFPE molds at various sputtering times from 0 s to 180 s. The width of the nanoridges on the PFPE mold was 125 nm, and the period was 500 nm.

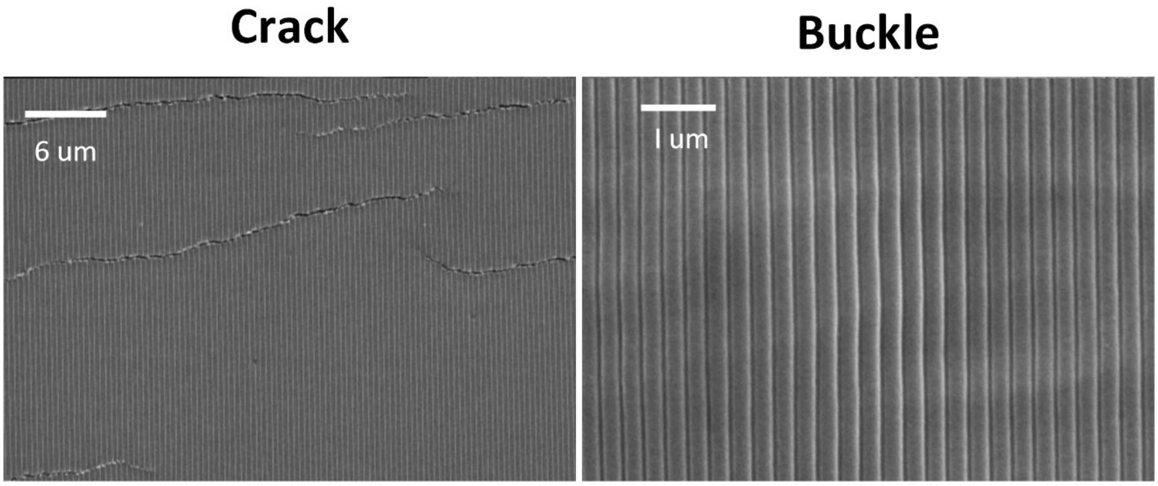

Fig. S4 Top-view SEM images of the defects (i.e., crack and buckle) that were produced by the high thermal stress applied on the PFPE surface by one-step gold sputtering.

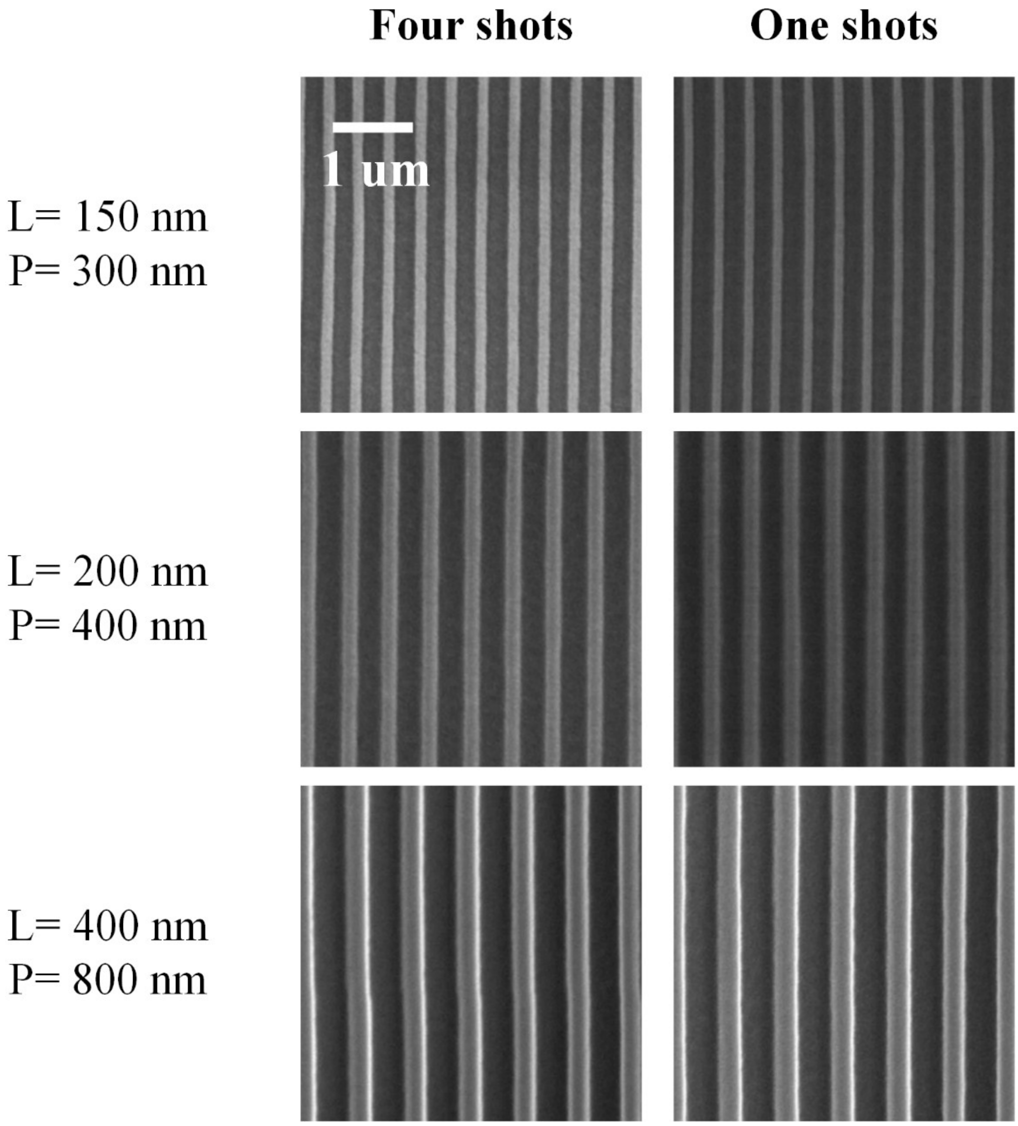

Fig. S5 SEM images of the nano-ridge PFPE surfaces coated with 40 nm gold. PFPE molds with ridge widths of 150 nm, 200 nm, and 400 nm were used. The duty ratios (width to period ratio) of nano-ridges were fixed at 0.5. One-step and four-step sputtering processes were compared.

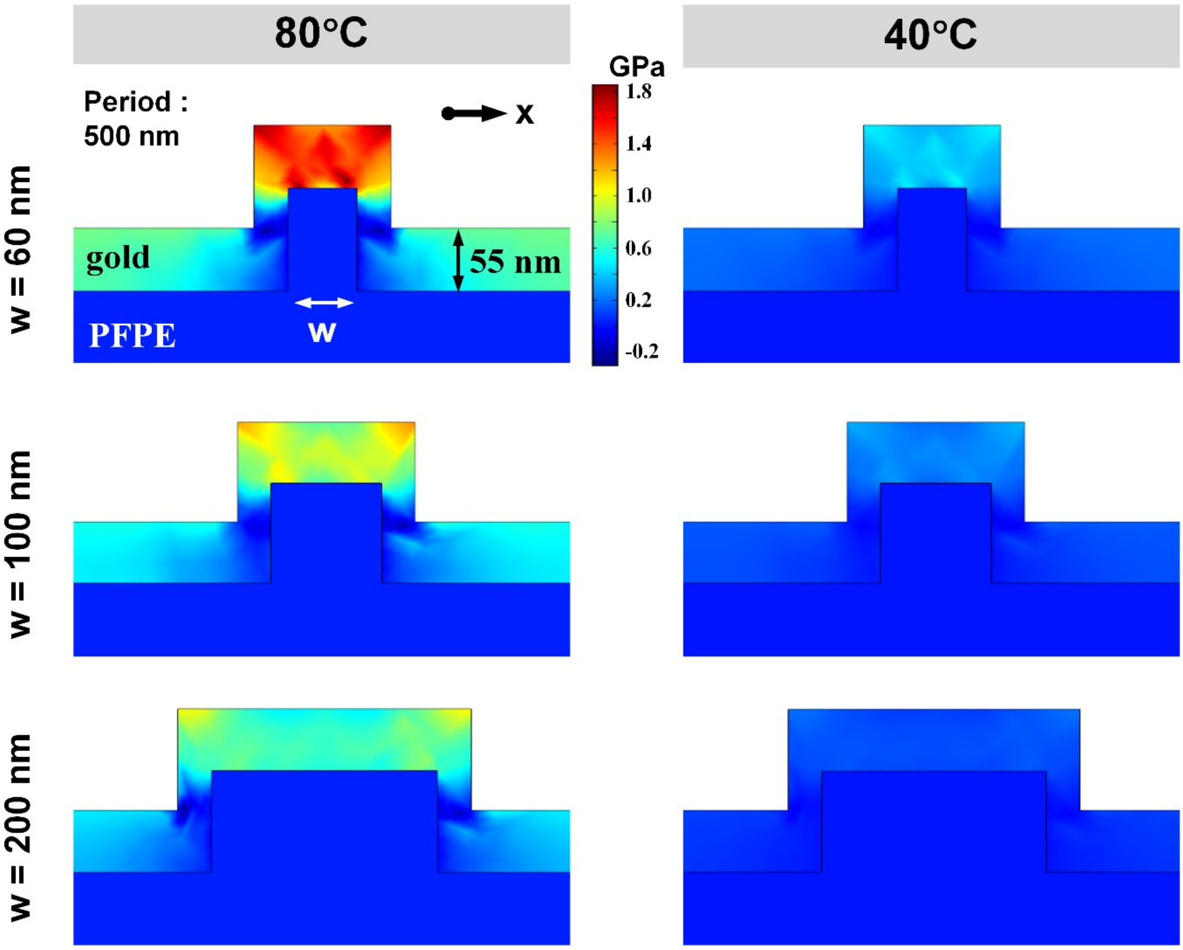

Parameter	Gold	PFPE
Young's modulus (GPa)	550 [1]	0.0405
Poisson's ratio	0.42	0.49
Density (kg/m^3)	19300	1000
Coefficient of thermal expansion (1/K)	1.42 x 10^{-5}	3 x 10^{-4}

Fig. S6 Thermal stress distribution of 55 nm gold film coated on PFPE nano-ridges analyzed by finite element method. The PFPE nano-ridges with ridge a width (w) of 60 nm, 100 nm and 200nm were compared. Temperature of the sample was assumed to be 40°C and 80°C, respectively. The period and height of nano-ridges are 500 nm and 90 nm. The parameters used in the simulation are listed in the above table.

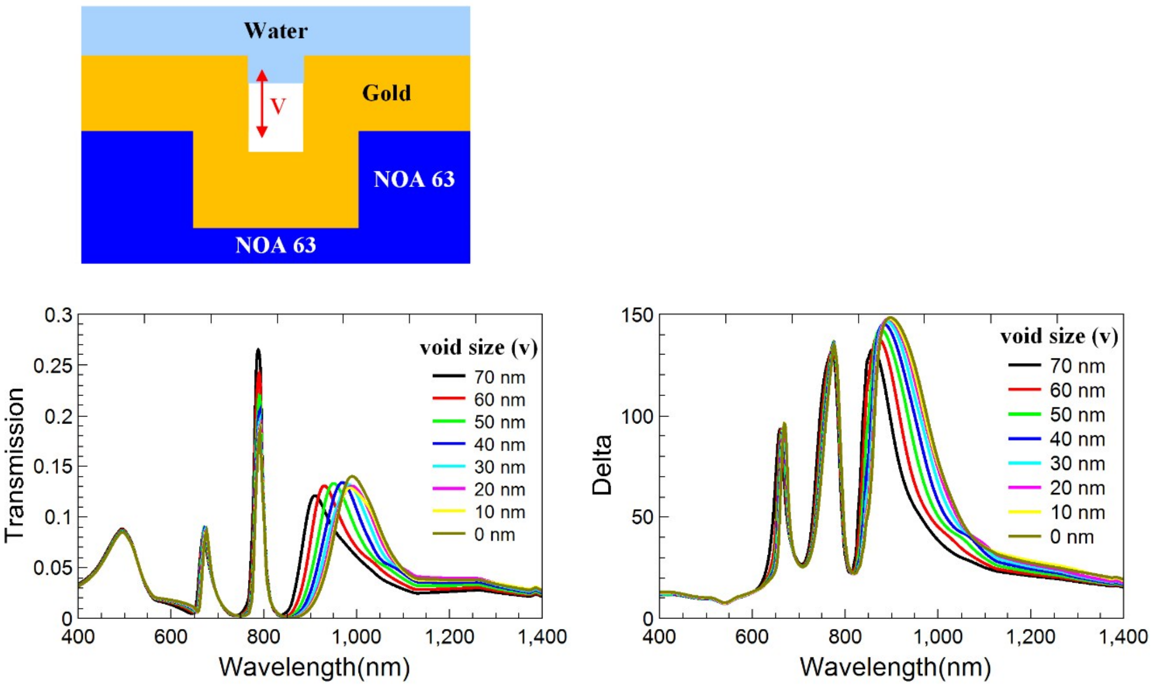

Fig. S7 Simulated transmission and phase spectra of the nano-pleat array immersed in water with the air void height (v) ranging from 0 to 70 nm.

Measured transmission spectra of fabricated nano-pleat arrays with various periods

Figs. S8(a) and S8(b) show the measured transmission spectra of fabricated nano-pleat arrays in air and water, respectively. The periods were 400, 500, and 600 nm. The cavity width and cavity depth were 40 and 79 nm, respectively. For the array with a period of 400 nm, a peak caused by the +1st coupling mode at the NOA63 side appeared at 612 nm. The broad peak at 758 nm was the cavity mode. The trend of the spectrum was consistent with that of the simulated spectrum in Fig. 4(a). The resonant wavelength of the +1st coupling mode at the NOA63 side moved to 763 nm when the period was 500 nm. The wavelengths of +1 W_{NOA63} and +1 BW-SPP_{NOA63} were close to that of the cavity mode, resulting in improved coupling efficiency with enhanced transmission. The cavity mode red-shifted to 873 nm because of the coupling mode. The coupling mode further moved across the cavity mode toward the longer wavelength as the period increased to 600 nm. The resonant wavelength was 910 nm. The coupling efficiency was reduced with a lower transmission peak because the coupling mode was far from the cavity mode at this period.

The +1st coupling mode at the water side was not observed for the array with a period of 400 nm when the sample was immersed in water [Fig. S8(b)]. The wavelength of the coupling mode was close to the region of the gold interband transition.[2] No transmitted signal was observed because of the strong absorption of the gold in this region. The coupling modes at the water side appeared at 656 and 815 nm when the grating period increased to 500 and 600 nm, respectively. These results were consistent with the trends of the simulated spectra in Fig. 4(b). The coupling mode of the 500-nm period was close to the visible wavelength region, which can be easily detected by a silicon detector. Moreover, the transmission peak of the coupling mode was stronger at this period. Therefore, we focused on the nano-pleat array with a period of 500 nm.

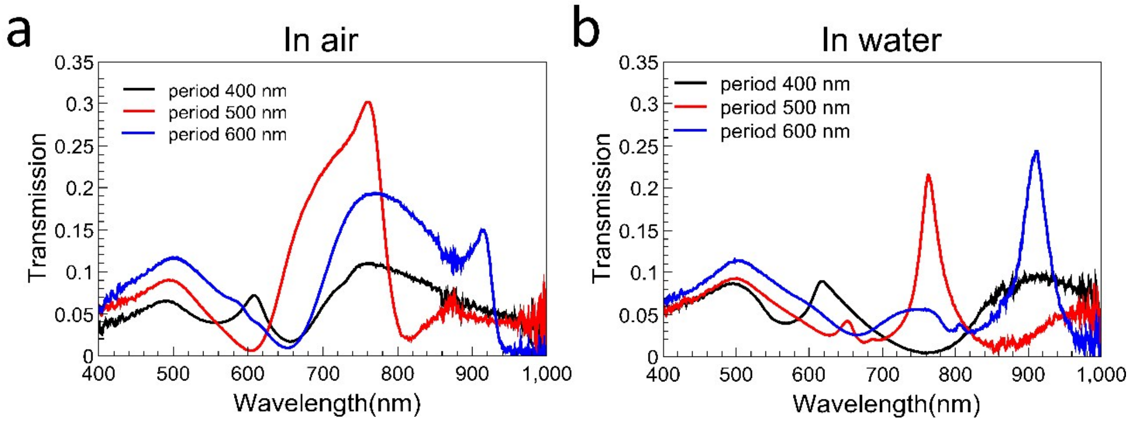

Fig. S8 Measured transmission spectra of nano-pleat arrays with periods of 400, 500, and 600 nm in (a) air and (b) water. The nano-pleat arrays have a cavity width of 40 nm and a cavity depth of 70 nm.

Near-field distributions of the cavity mode and coupling modes in nano-pleat arrays

We employed RCWA to calculate the near-field distributions of E_x, E_z, and H_y fields at the x-z plane (Fig. S9). For the cavity mode of the freestanding nano-pleat array in air [black spectrum in Fig. 3(b)], strong E_x and H_y fields were found inside the nanocavity at 798 nm. The E_z field is localized at the corner of the cavity top and the cavity bottom. Power flow is illustrated in the H_y field plot, as shown in Fig. S10. The blue arrows indicate the direction of the energy flow, and the arrow length represents the energy strength. The energy flows into the nanocavities of the nano-pleat array. In the cavity mode, the E_x field concentrates at the top of the nanocavity, and the H_y field resides at the bottom of the nanocavity, which is consistent with previous studies.[3-5]

For the coupling mode at the water side (peak 1) of freestanding nano-pleat array in water [blue spectrum in Fig. 3(b)], strong E_x field exists inside the nanocavity, and the E_z field distributes at the top of the metal surface and decays with the distance from the surface. H_y field resides in the nanocavity and on top of the metal surface. The interplay between WA, BW-SPP, and cavity mode could contribute to this resonance peak.

For the coupling mode at the NOA 63 side (peak 2) of non-freestanding nano-pleat array in water [red spectrum in Fig. 3(b)], E_x field resides in the upper nanocavity, E_z field distributes at the bottom of the metal surface, and H_y field distributes in the lower cavity and the bottom of upper cavity. This phenomenon indicates that peak 2 is formed by coupling the cavity mode with +1st WA_{NOA63} and +1st $BW\text{-}SPP_{NOA63}$. A broad peak of the cavity mode appears at 1014 nm, which is slightly red-shifted compared with that of the freestanding nano-pleat array. The redshift of the cavity mode is caused by the appearance of peak 2.

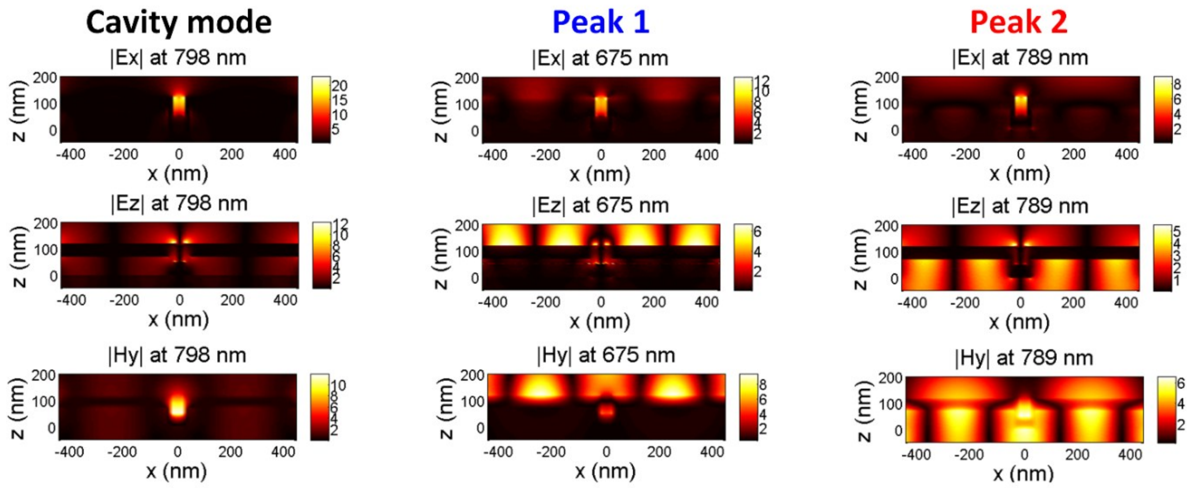

Fig. S9 Near-field distributions of the cavity mode, the coupling modes at the water side (peak 1) and NOA 63 side (peak 2).

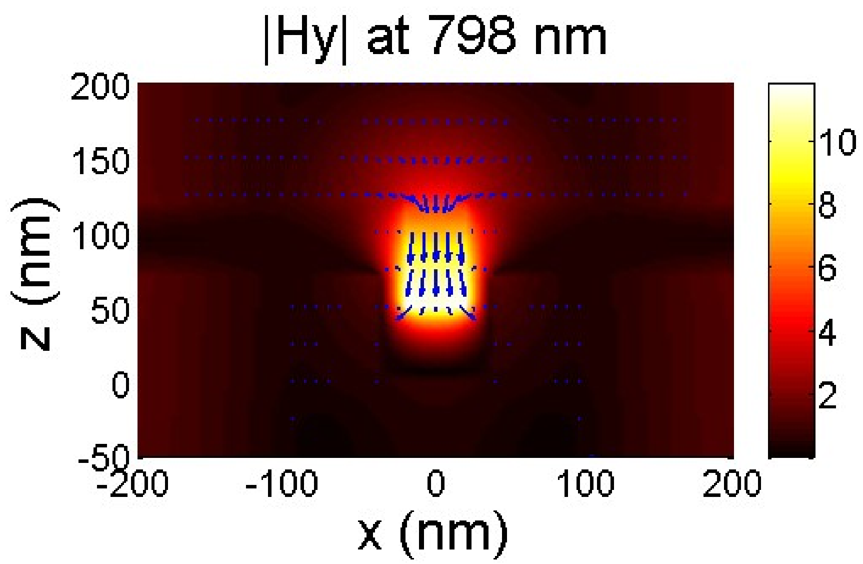

Fig. S10 Power flow of light funneled into the nanocavities of the nano-pleat array.

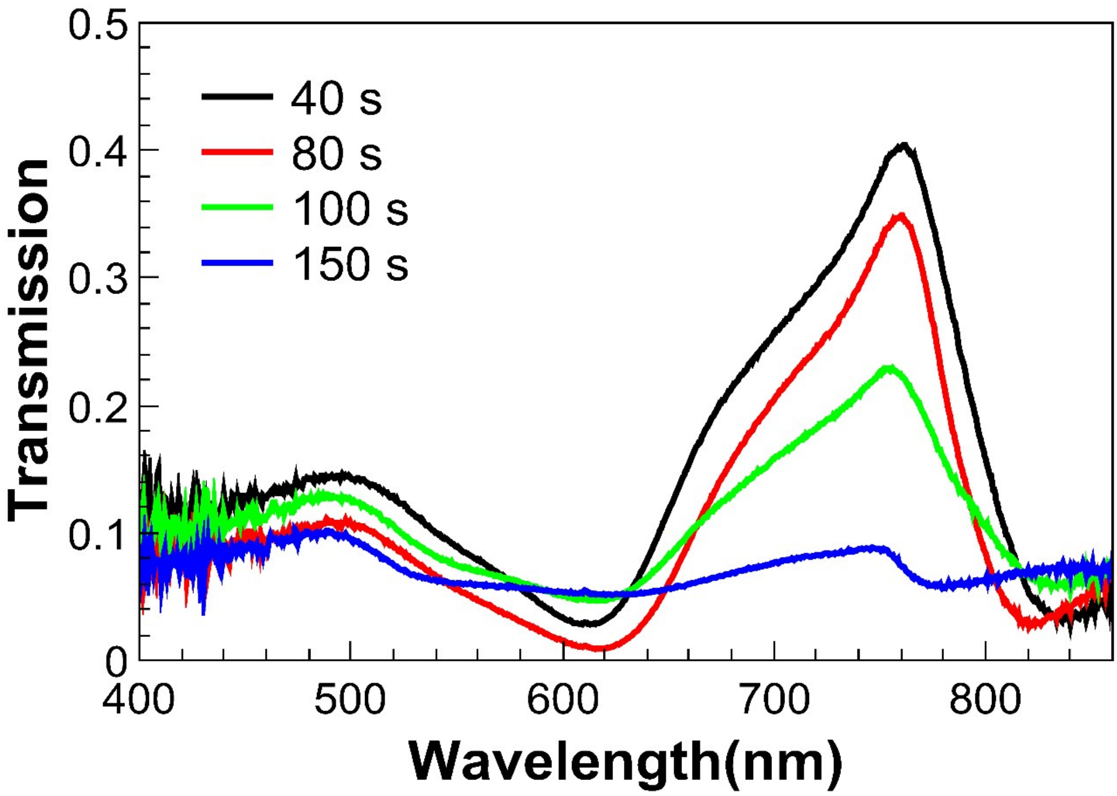

Fig. S11 Measured transmission and phase spectra of the nano-pleat arrays with various NOA63 filling levels in water. The nano-pleat arrays have a cavity width of 40 nm and a cavity depth of 70 nm.

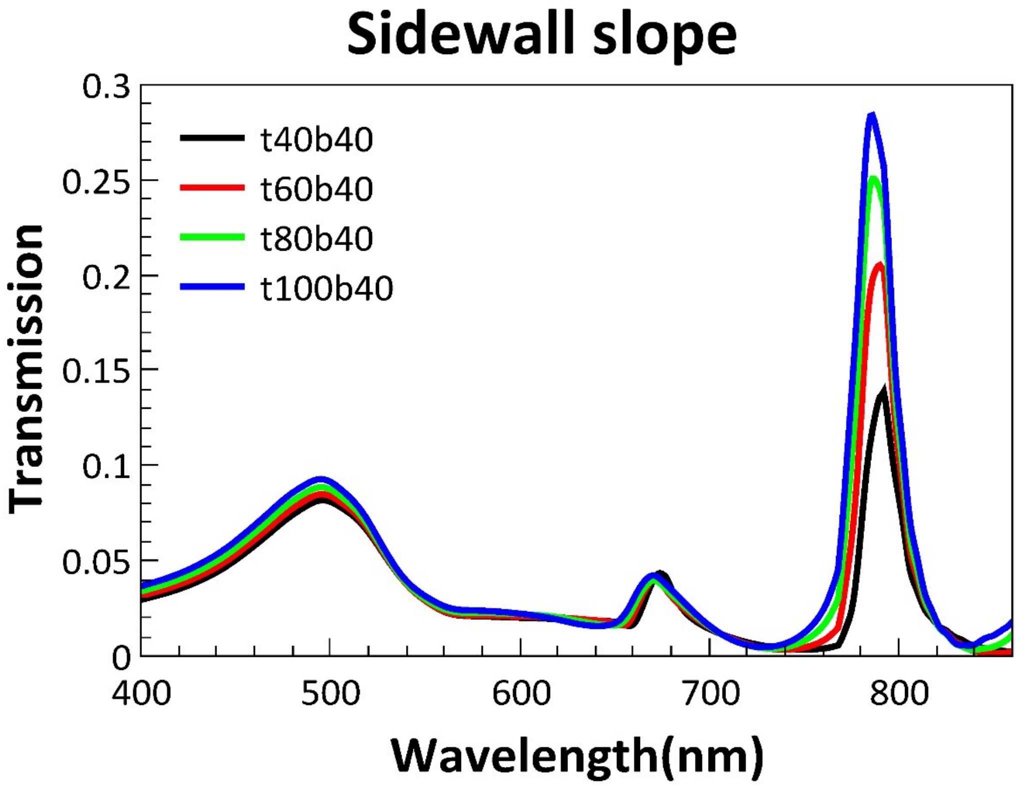

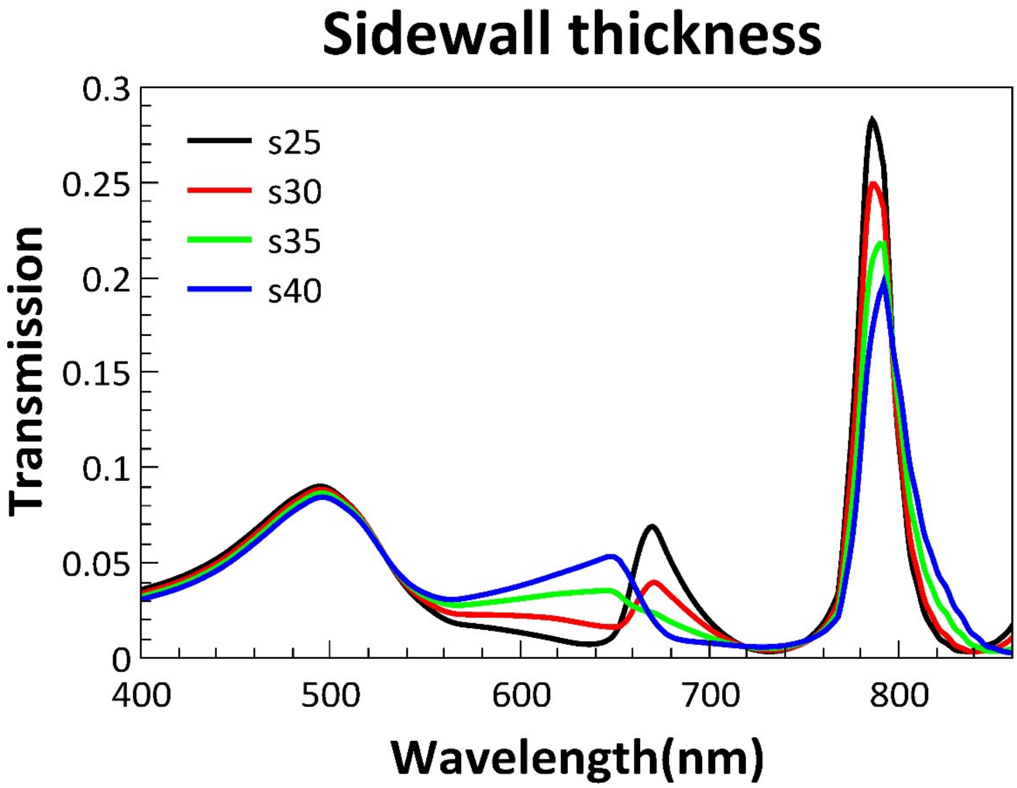

Fig. S12 Simulated transmission spectra of the nano-pleat arrays with various sidewall slopes and sidewall thicknesses.

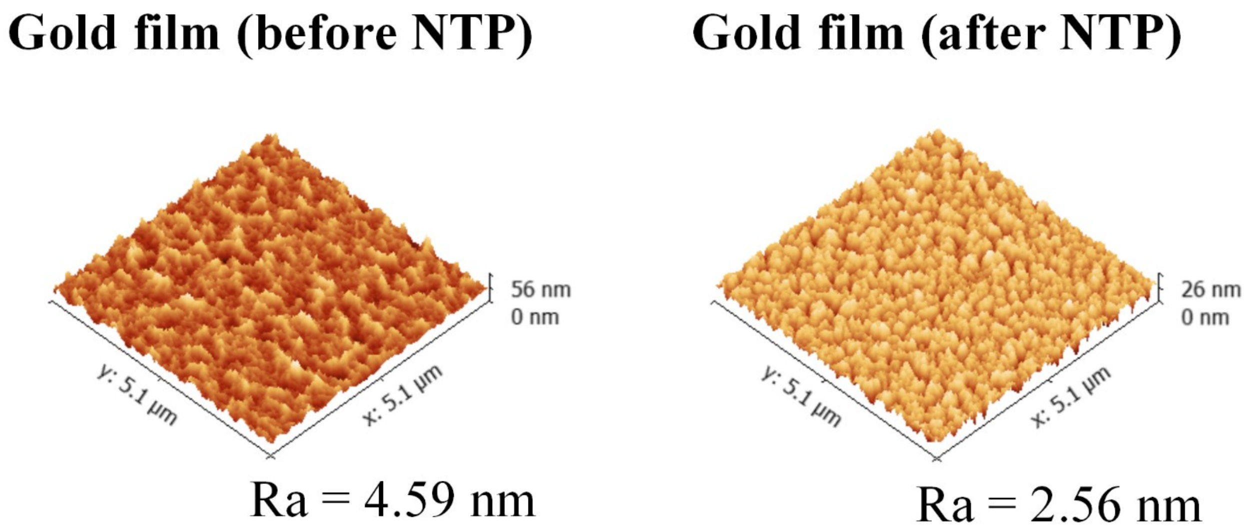

Fig. S13 AFM images of gold film surface before NTP and after NTP.

Reference

[1] F. Avilés, L. Llanes and A. Oliva, *Journal of materials science*, 2009, 44, 2590-2598.

[2] M. H. Lee, H. Gao, T. W. Odom, *Nano Letters* **2009**, *9*, 2584.

[3] S. Kim, Y. Xuan, V. P. Drachev, L. T. Varghese, L. Fan, M. Qi, K. J. Webb, *Opt. Express* **2013**, *21*, 15081.

[4] H. T. Miyazaki, Y. Kurokawa, *Applied Physics Letters* **2006**, *89*, 211126.

[5] Y.-K. R. Wu, A. E. Hollowell, C. Zhang, L. J. Guo, *Scientific reports* **2013**, *3*, 1194.